

# Helix Angle Effect on the Helical Gear Load Carrying Capacity

Mehmet Bozca

Machine Design Division, Mechanical Engineering Faculty, Yildiz Technical University, Istanbul, Turkey

Email: mbozca@yildiz.edu.tr

**How to cite this paper:** Bozca, M. (2018) Helix Angle Effect on the Helical Gear Load Carrying Capacity. *World Journal of Engineering and Technology*, 6, 825-838. <https://doi.org/10.4236/wjet.2018.64055>

**Received:** September 4, 2018

**Accepted:** November 13, 2018

**Published:** November 16, 2018

Copyright © 2018 by author and Scientific Research Publishing Inc.

This work is licensed under the Creative Commons Attribution International License (CC BY 4.0).

<http://creativecommons.org/licenses/by/4.0/>



Open Access

## Abstract

The aim of this study is to investigate the helix angle effect on the helical gear load carrying capacity, including the bending and contact load carrying capacity. During the simulation, the transverse contact ratio is calculated with respect to the constant pressure angle. By changing the helix angle, both the overlap contact ratio and total contact ratio are calculated and simulated. The bending stress and contact stress of a helical gear are calculated and simulated with respect to the helix angle. Solid (CAD) modelling of a pinion gear was obtained using SOLIDWORKS software. The analytically obtained results and finite elements method results are compared. It is observed that increasing the helix angle causes an increase of the contact ratio of the helical gear. Furthermore, increasing the contact ratio reduces the bending stress and contact stress of the helical gear. However, with a constant transverse contact ratio, it is possible to improve the total contact ratio depending on the helix angle. It is concluded that a higher helix angle increases the helical gear bending and contact load carrying capacity.

## Keywords

Helical Gear, Helix Angle, Contact Ratio, Bending Stress, Contact Stress

## 1. Introduction

Gears are widely used to mechanically transmit power in automotive transmissions. The aim of the gears is to couple two shafts together; the rotation of the drive-shaft is a function of the rotation of the drive-shaft in the gear mechanism. Therefore, determining the geometric design parameters of gears is crucial.

The contact ratio is an important parameter for successful gear design. The helix angle is considered to be an effective parameter to increase the contact ratio of a helical gear. Thus, it is possible to increase the helical gear load carrying

capacity, including the tooth bending stress and tooth contact stress.

One of the disadvantages of increasing the helix angle is the axial forces caused on the helical gear mechanism.

Optimisation of effective design parameters to reduce the tooth bending stress in an automotive transmission gearbox is presented. Therefore, the contact ratio effect on the tooth bending stress by changing the contact ratio with respect to the pressure angle is analysed [1]. It is concluded that a higher contact ratio results in reduced tooth bending stress, while a higher pressure angle and decreased contact ratio caused an increase in tooth bending stress and contact stress [1].

When the helix angle is increased from 15 [°] to 35 [°], the corresponding bending stress and compression stress decrease [2].

It was concluded that a helix angle increase had significant effects on the tooth-root bending stress and tooth compressive stress. Moreover, it was observed that when the helix angle increased from 0 [°] to 22.5 [°], both the bending stress and compression stress were reduced approximately 10% [3].

For a given number of teeth, a smaller pressure angle may produce an undercut. However, the contact ratio increases, so the load carrying capacity may improve as the load is distributed along a longer line of contact [4].

The contact ratio for a helical gear pair increases with the helix angle, which generates the screwed surface of the tooth face [5].

The aim of this study is to investigate the helix angle effect on the helical gear load carrying capacity, including the bending and contact load carrying capacity. For this aim the analytically obtained results and finite elements method results are compared. It is concluded that a higher helix angle increases the helical gear bending and contact load carrying capacity.

## 2. Method

### 2.1. Pinion and Wheel Gears Mechanism

In the proposed pinion and wheel gear mechanism, all pinion and wheel gears are helical and are made of 16MnCr5.

#### 2.1.1. Helix Angle $\beta$

The helix angle,  $\beta$ , is the angle between the helix line and horizontal axis, as shown in **Figure 1**.

#### 2.1.2. Contact Ratio

The dimensions of the helical gear are shown in **Figure 2**, and the contact line of the helical gear is shown in **Figure 3**.

A second pair of mating teeth should come into contact before the first pair is out of contact during pinion and wheel gear running [6].

If the gear contact ratio is equal to 1, one tooth is leaving contact just as the next tooth is beginning contact. If the gear contact ratio is larger than 1, load sharing among the teeth is possible during pinion and wheel gear running [7].

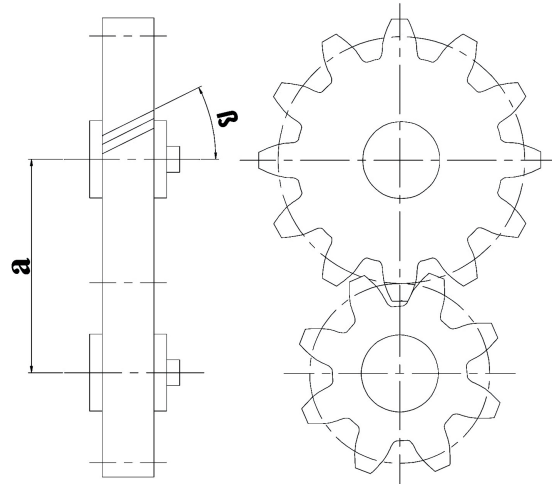


**Figure 1.** Pinon and wheel gear mechanism.

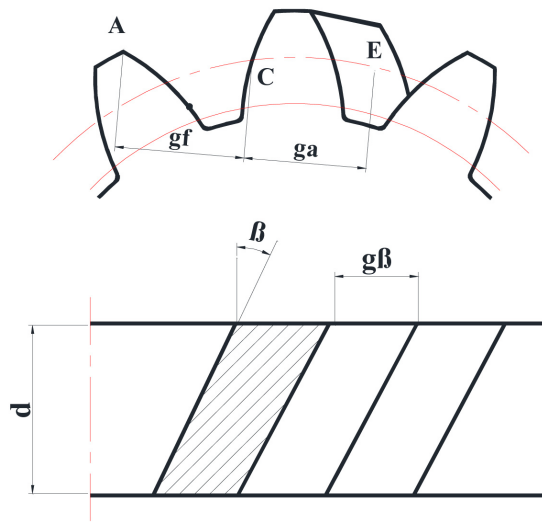


**Figure 2.** Dimensions of a helical gear.

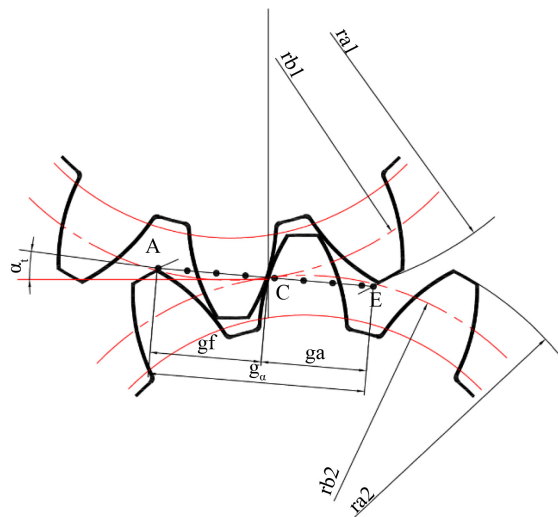


**Figure 3.** Contact line of a helical gear.

When the contact ratio is equal to 2 or more, at least two pairs of teeth are theoretically in contact [7].

If the gear profile contact ratio is less than 2.0, it is called the Low Contact Ratio (LCR). If the gear profile contact ratio equals 2.0 or greater, it is called the High Contact Ratio (HCR).

The contact ratio consists of two parts, such as the transverse contact ratio,  $\varepsilon_\alpha$ , and the overlap or face contact ratio,  $\varepsilon_\beta$ .

#### 1) Transverse contact ratio $\varepsilon_\alpha$

It is well-known that the average number of teeth that are in contact as the gears rotate is the contact ratio (CR). The contact ratio is calculated from the following equation.

The transverse contact ratio,  $\varepsilon_\alpha$  is calculated as follows [8] [9] [10] [11].

$$\varepsilon_\alpha = \frac{g_\alpha}{p_{et}} \quad (1)$$

$$\varepsilon_\alpha = \frac{0.5 \cdot \left( \sqrt{d_{a1}^2 - d_{b1}^2} + \sqrt{d_{a2}^2 - d_{b2}^2} \right) - a_d \cdot \sin \alpha_t}{\pi \cdot m_t \cdot \cos \alpha_t} \quad (2)$$

where  $g_\alpha$  is the path length of the contact line [mm],  $p_{et}$  is the base pitch [mm],  $d_{a1}$  is the addendum circle diameter of the pinion gear [mm],  $d_{b1}$  is the base circle diameter of the pinion gear [mm],  $d_{a2}$  is the addendum circle diameter of the wheel gear [mm],  $d_{b2}$  is the base circle diameter of the wheel gear [mm],  $a_d$  is the centre distance [mm],  $\alpha_t$  is the transverse pressure angle [°], and  $m_t$  is the transverse module [mm].

#### 2) Overlap ratio $\varepsilon_\beta$

The overlap ratio,  $\varepsilon_\beta$  is calculated as follows [8] [9] [10] [11].

$$\varepsilon_\beta = \frac{U}{p_t} \quad (3)$$

$$\varepsilon_\beta = \frac{b \cdot \tan \beta}{p_t} \quad (4)$$

$$\varepsilon_\beta = \frac{b \cdot \sin \beta}{\pi \cdot m_n} \quad (5)$$

where  $U$  is the action length [mm],  $p_t$  is the transverse pitch [mm],  $b$  is the face width [mm], and  $m_n$  is the normal module [mm].

#### 3) Total contact ratio $\varepsilon_\gamma$

The total contact ratio,  $\varepsilon_\gamma$  is calculated as follows.

$$\varepsilon_\gamma = \varepsilon_\alpha + \varepsilon_\beta \quad (6)$$

where  $\varepsilon_\alpha$  is the transverse contact ratio and  $\varepsilon_\beta$  is the overlap ratio. Helical gears have higher load carrying capacities than spur gears because their contact ratios are larger than those of spur gears.

## 2.2. Calculating the Load Carrying Capacity of Helical Gears

### 2.2.1. Nominal Tangential Load

The nominal tangential load  $F_t$  is calculated as follows.

$$F_t = \frac{2 \cdot T_L}{d_1} \quad (7)$$

where  $T_L$  is the applied torque [N·mm] and  $d_1$  is the base diameter of the tooth diameter [mm].

### 2.2.2. Axial Load

Axial load  $F_a$  is calculated as follows.

$$F_a = \frac{F_t}{\tan \beta} \quad (8)$$

where  $\beta$  is helix angle [°].

### 2.2.3. Tooth Bending Stress

The real tooth-root stress,  $\sigma_F$  is calculated as follows [8] [9] [10] [11] [12]. The bending stress of the tooth-root is shown in **Figure 4**.

$$\sigma_F = \frac{F_t}{b m_n} Y_F Y_S Y_\varepsilon Y_\beta K_A K_V K_{F\beta} K_{F\alpha} \quad (9)$$

where  $F_t$  is the nominal tangential load [N],  $b$  is the face width [mm],  $m_n$  is the normal module [mm],  $Y_F$  is the form factor [-],  $Y_S$  is the stress correction factor [-],  $Y_\varepsilon$  is the contact ratio factor [-],  $K_A$  is the application factor [-],  $K_V$  is the internal dynamic factor [-],  $K_{F\beta}$  is the face load factor for tooth-root stress [-] and  $K_{F\alpha}$  is the transverse load factor for tooth-root stress [-]. The safety factor for bending stress  $S_F$  is calculated as follows [8] [9] [10] [11] [12].

$$S_F = \frac{\sigma_{Fp}}{\sigma_F} \quad (10)$$

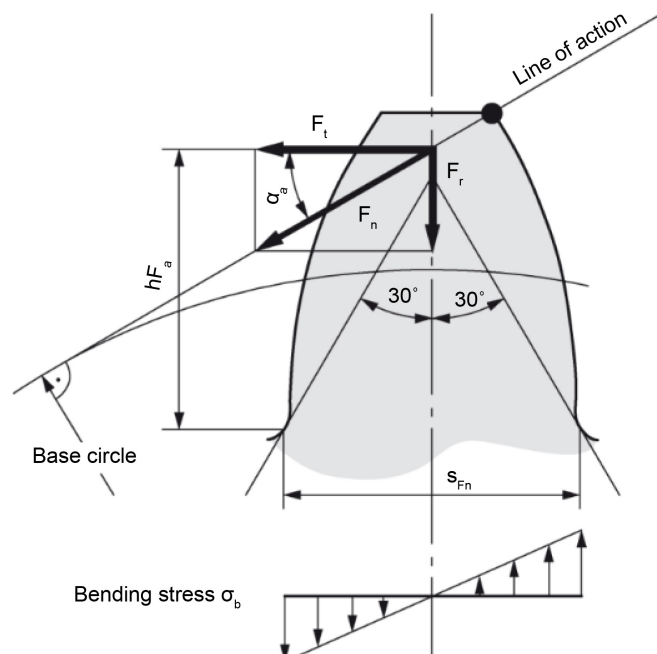


**Figure 4.** Bending stress at the tooth root.

where  $\sigma_{fp}$  is the permissible bending stress.

#### 2.2.4. Tooth Contact Stress

The real contact stress,  $\sigma_H$  is calculated as follows [8] [9] [10] [11] [12]. The contact stress at the tooth flank is shown in **Figure 5**.

$$\sigma_H = \sqrt{\frac{F_t}{bm_n} \frac{u+1}{u}} Z_H Z_E Z_\epsilon Z_\beta \sqrt{K_A K_V K_{H\beta} K_{H\alpha}} \quad (11)$$

where  $u$  is the gear ratio [-],  $Z_H$  is the zone factor [-],  $Z_E$  is the elasticity factor [ ],  $Z_\epsilon$  is the contact ratio factor [-],  $Z_\beta$  is the helix angle factor [-],  $K_{H\beta}$  is the face load factor for contact stress [-] and  $K_{H\alpha}$  is the transverse load factor for contact stress [-].

The safety factor for contact stress,  $S_H$  is calculated as follows [8] [9] [10] [11] [12].

$$S_H = \frac{\sigma_{Hp}}{\sigma_H} \quad (12)$$

where  $\sigma_{Hp}$  is the permissible contact stress.

### 2.3. Finite Elements Model

Solid (CAD) modelling of a pinion gear was obtained using SOLIDWORKS software. A solid model is essential for finite element method (FEM) analysis [13] [14]. Solid (CAD) modelling of a pinion gear is shown in **Figure 6**.

#### Finite Element Analysis

The obtained Solid (CAD) model is used to obtain the finite element method (FEM) model using the SOLIDWORKS finite element tool.

##### 1) Boundary conditions

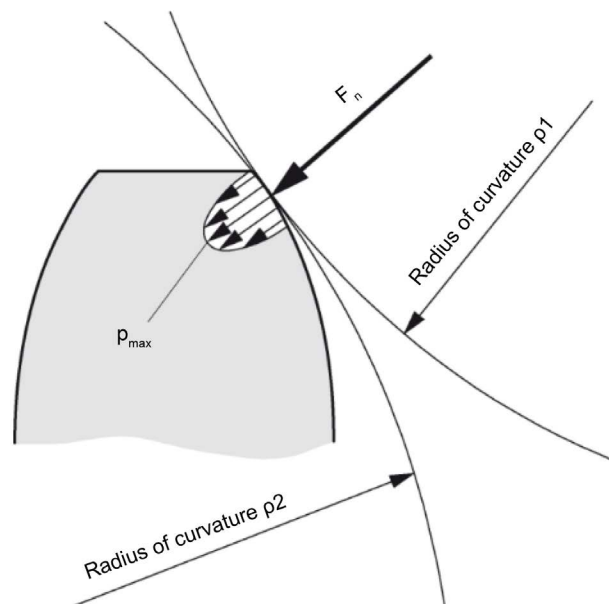


**Figure 5.** Contact stress at the tooth flank.



**Figure 6.** Solid (CAD) modelling of a pinion gear.

To simulate the actual conditions of the pinion gear for analysis, the boundary conditions below were used.

- a) The pinion gear was constrained in the centre of the pinion gear.
- b) The applied load for bending the pinion gear tooth was considered at the tooth top surface.

### 3. Numerical Example

During simulation, the tooth bending stress and tooth contact stress were calculated according to ISO 6336. The effects of the helix angle on the tooth bending stress and tooth contact stress are analysed by varying the helix angle. The tooth bending stress and tooth contact stress parameters are shown in **Table 1**.

The tooth bending stress and tooth contact stress simulation results are shown in **Table 2**.

#### 3.1. Helix Angle and Overlap Contact Ratio Relation

The helix angle and overlap contact ratio relation are shown in **Figure 7**. As the helix angle increases from 22 [°] to 32 [°], the overlap contact ratio increases from 1.01 [-] to 1.43 [-].

#### 3.2. Helix Angle and Total Contact Ratio Relation

The helix angle and total contact ratio relation are shown in **Figure 8**. As the helix angle increases from 22 [°] to 32 [°], the total contact ratio increases from 2.52 [-] to 2.88 [-].

#### 3.3. Helix Angle and Bending Stress Relation

The helix angle and tooth bending stress relation are shown in **Figure 9**. As the helix angle decreases from 22 [°] to 12 [°], the bending stress is reduced from 365 [N/mm<sup>2</sup>] to 233 [N/mm<sup>2</sup>].

**Table 1.** Tooth bending stress and tooth contact stress parameters.

Parameters	Value	Unit
Torque $T_L$	$260 \times 10^3$	[N·mm]
Gear ratio $u$	1.814	[-]
Module $m$	4	[mm]
Number of teeth $z$	21	[-]
Face width $b$	34	[mm]
Form factor $Y_F$	2.87	[-]
Stress correction factor $Y_S$	1.6	[-]
Application factor $K_A$	1.25	[-]
Dynamic factor $K_V$	1.14	[-]
Transverse load factor $K_{Fa}$	1.2	[-]
Nominal stress number $\sigma_{FLim}$	350	[N/mm <sup>2</sup> ]
Life factor $Y_N$	1	[-]
Relative notch sensitivity factor $Y_\delta$	1	[-]
Relative surface factor $Y_R$	1	[-]
Size factor $Y_X$	1	[-]
Zone factor $Z_H$	2.36	[-]
Elasticity factor $Z_E$	189.8	[N/mm <sup>2</sup> ] <sup>1/2</sup>
Transverse load factor $K_{Ha}$	1.2	[-]
Allowable stress number $\sigma_{HLim}$	1400	[N/mm <sup>2</sup> ]
Life factor $Z_N$	1	[-]
Roughness factor $Z_R$	1	[-]
Work hardening factor $Z_W$	1	[-]
Size factor $Z_X$	1	[-]

**Table 2.** Tooth bending stress and tooth contact stress simulation results.

Helix angle $\beta$ [°]	Overlap contact ratio $\epsilon_\beta$ [-]	Total contact ratio $\epsilon_\gamma$ [-]	Tooth bending stress $\sigma_F$ [N/mm <sup>2</sup> ]	Tooth contact stress $\sigma_H$ [N/mm <sup>2</sup> ]
22	1.01	2.52	365	1265
24	1.10	2.60	340	1241
26	1.19	2.67	314	1215
28	1.27	2.74	287	1188
30	1.35	2.81	260	1159
32	1.43	2.88	233	1128

### 3.4. Helix Angle and Tooth Contact Stress Relation

The helix angle and contact stress relation are shown in **Figure 10**. As the helix angle decreases from 22 [°] to 12 [°], the bending stress is reduced from 1265 [N/mm<sup>2</sup>] to 1128 [N/mm<sup>2</sup>].

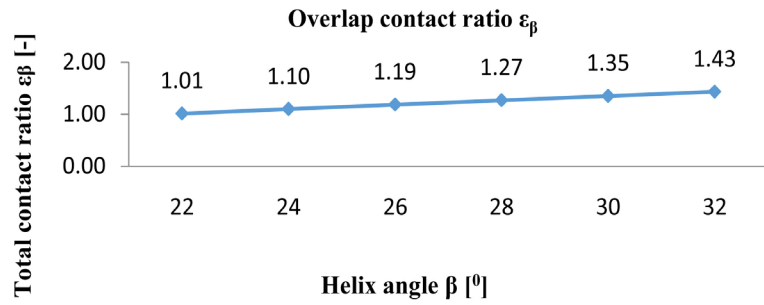


Figure 7. Helix angle and overlap contact ratio relation.

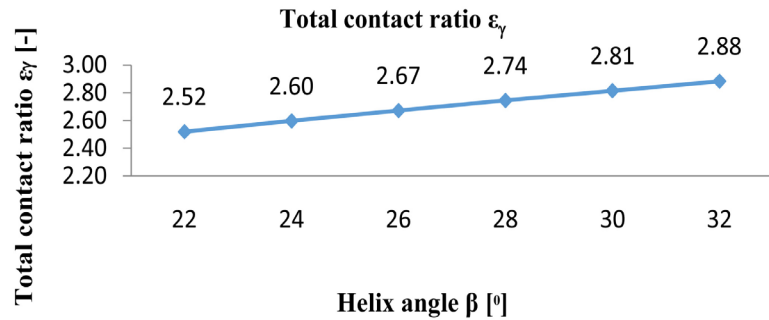


Figure 8. Helix angle and total contact ratio relation.

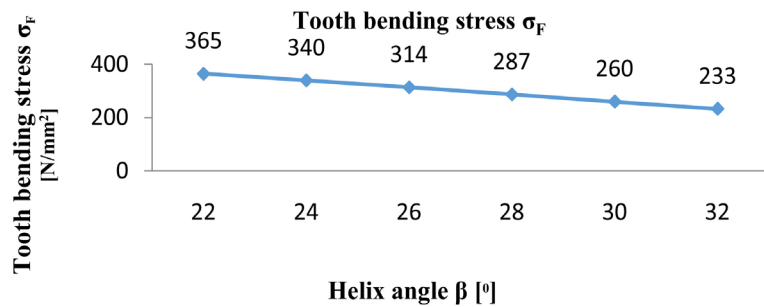


Figure 9. Helix angle and tooth bending stress relation.

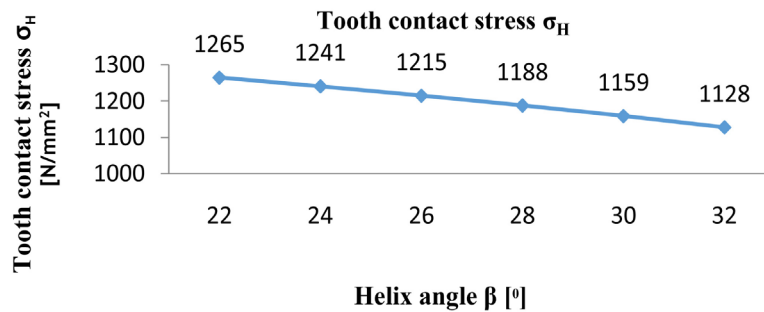
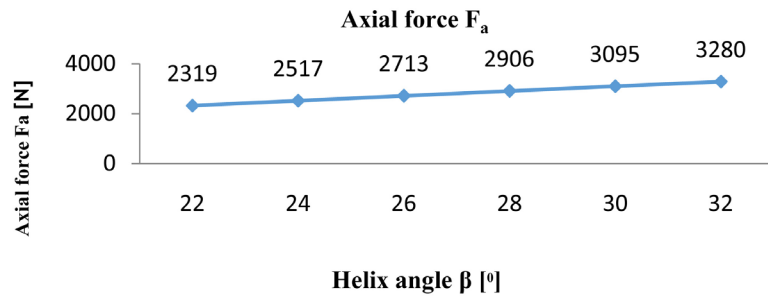


Figure 10. Helix angle and tooth contact stress relation.

### 3.5. Helix Angle and Axial Force Relation

The helix angle and axial force relation is shown in Figure 11. As the helix angle decreases from 22 [°] to 12 [°], the axial force is increased from 2319 [N] to 3280 [N].



**Figure 11.** Helix angle and axial force relation.

### 3.6. Static Structural Analysis with FEM

Static structural analysis of the pinion gear was completed for the applied load considering the Von Mises stress. The Von Mises stress is written as follows.

$$\sigma_{vM} = \sqrt{\sigma^2 + 3\tau^2} \quad (13)$$

Theoretical bending stress is written as follows.

$$\sigma_{FT} = \frac{F_t}{b \cdot m} Y_F \quad (14)$$

#### 3.6.1. Applied Load

The applied load was considered in 6 different pinion gears that had 6 different helix angles. The Von-Mises stresses are shown in **Figures 12-17**.

#### 3.6.2. Solution

The Von Mises stress obtained by finite elements analyses are shown in **Table 3**. A comparison between Von Mises Stress with FEM and analytical static stress depending on the helix angle is shown in **Figure 12**. By observing obtained finite elements method results, it is concluded that 45% increased helix angle result in 6.5% decreased Von Mises stress.

The maximum Von Mises stress of the pinion gear reaches 112,900 [N/mm<sup>2</sup>] on the pinion tooth root for a helix angle  $\beta = 22$  [°], as shown in **Figure 13**.

The maximum Von Mises stress of the pinion gear reaches 112,340 [N/mm<sup>2</sup>] on the pinion tooth root for a helix angle  $\beta = 24$  [°], as shown in **Figure 14**.

The maximum Von Mises stress of the pinion gear reaches 111,236 [N/mm<sup>2</sup>] on the pinion tooth root for a helix angle  $\beta = 26$  [°], as shown in **Figure 15**.

The maximum Von Mises stress of the pinion gear reaches 110,348 [N/mm<sup>2</sup>] on the pinion tooth root for a helix angle  $\beta = 28$  [°], as shown in **Figure 16**.

The maximum Von Mises stress of the pinion gear reaches 108,242 [N/mm<sup>2</sup>] on the pinion tooth root for a helix angle  $\beta = 30$  [°], as shown in **Figure 17**.

The maximum Von Mises stress of the pinion gear reaches 105,984 [N/mm<sup>2</sup>] on the pinion tooth root for a helix angle  $\beta = 30$  [°], as shown in **Figure 18**.

## 4. Conclusions

During simulation, tooth bending stress and tooth contact stress were calculated according to ISO 6336. Solid (CAD) modelling of a pinion gear was completed

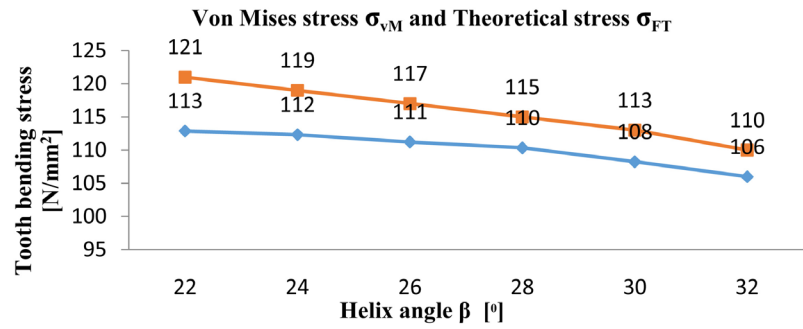


Figure 12. Comparison of Von Mises stress and Theoretical stress.

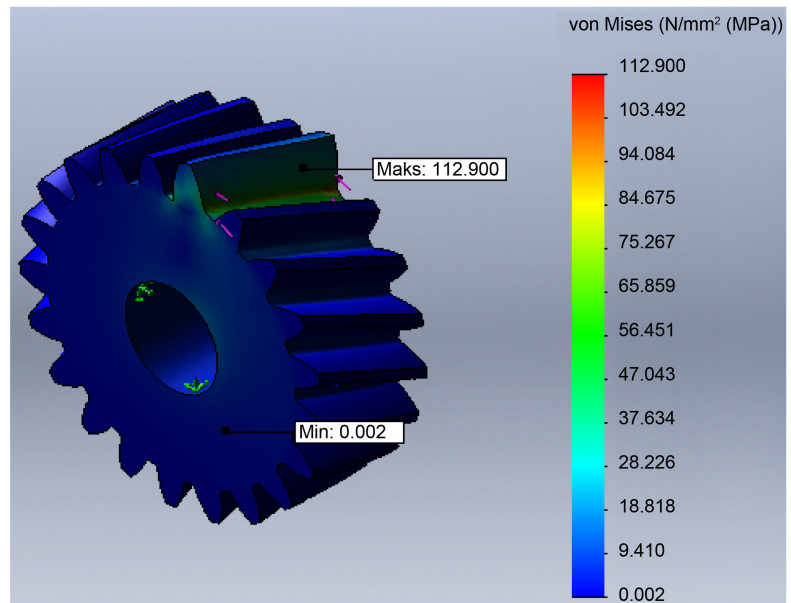


Figure 13. Von Mises stress for a helix angle  $\beta = 22$  [°].

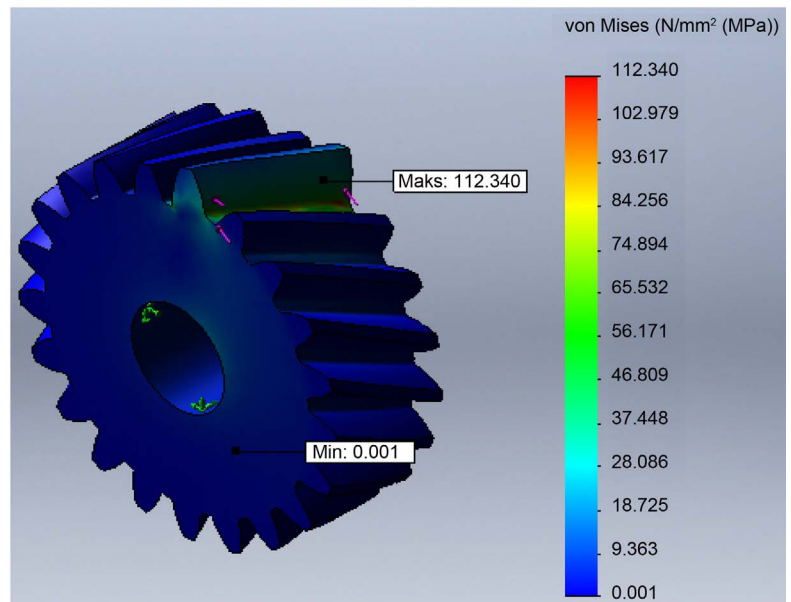


Figure 14. Von Mises stress for a helix angle  $\beta = 24$  [°].

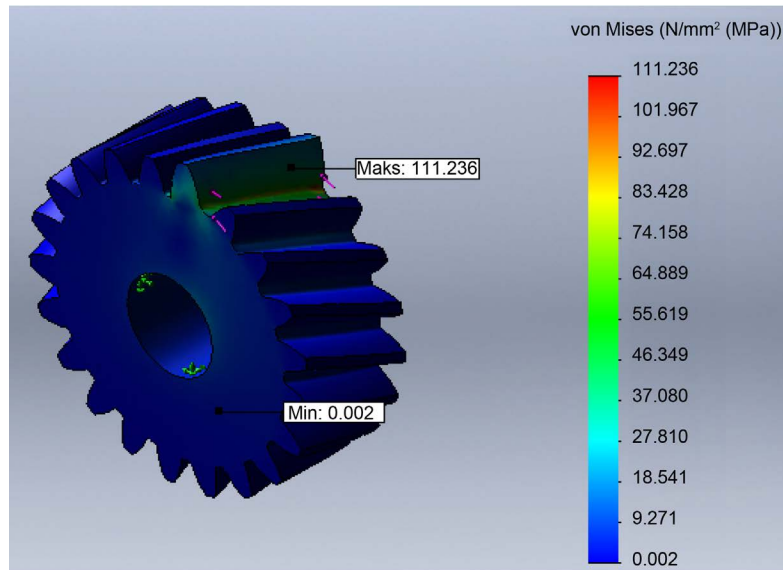


Figure 15. Von Mises stress for a helix angle  $\beta = 26$  [°].

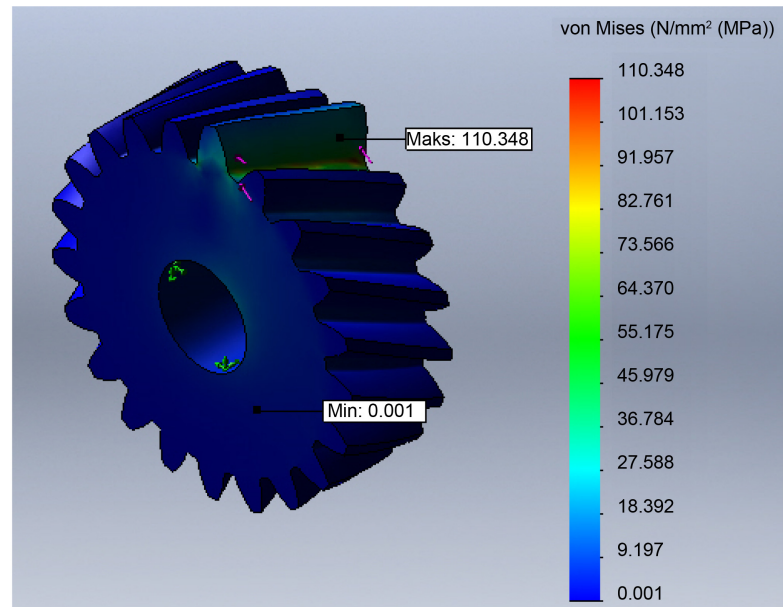


Figure 16. Von Mises stress for a helix angle  $\beta = 28$  [°].

using SOLIDWORKS software. The analytically obtained results and finite element method results were compared.

The effect of the helix angle on the tooth bending stress and tooth contact stress was analysed by varying helix angle, and the following conclusions are drawn.

Increasing the helix angle  $\beta$ , results in increasing the overlap contact ratio  $\epsilon_\beta$ . Thus, increasing the helix angle  $\beta$  results in increasing the total contact ratio  $\epsilon_\gamma$ .

Increasing the helix angle  $\beta$  results in a reduction of the tooth bending stress  $\sigma_F$  and tooth contact stress  $\sigma_H$ .

The analytically obtained results are verified by the finite element method

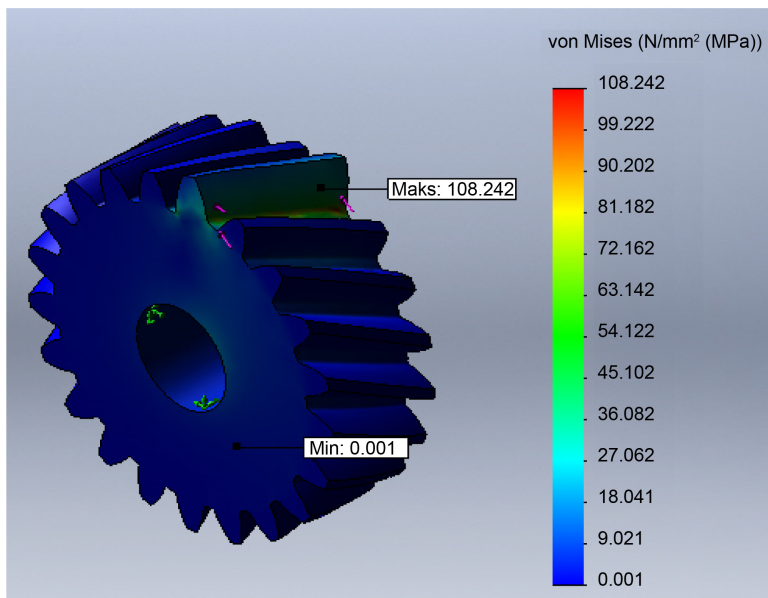


Figure 17. Von Mises stress for a helix angle  $\beta = 30$  [°].

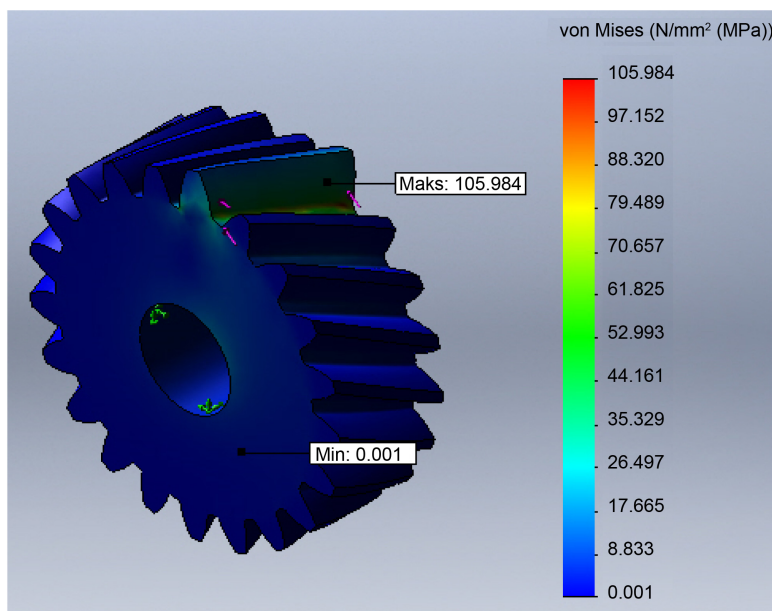


Figure 18. Von Mises stress for a helix angle  $\beta = 32$  [°].

Table 3. Von Mises stresses as determined by finite element analyses.

Helix angle $\beta$	Von Mises stress $\sigma_{VM}$	Theoretical bending stress $\sigma_{FT}$
$\beta = 22$	112,900	121,13
$\beta = 24$	112,340	119,35
$\beta = 26$	111,236	117,41
$\beta = 28$	110,348	115,34
$\beta = 30$	108,242	113,13
$\beta = 32$	105,984	110,79

results. By considering the tooth bending stress, the analytically obtained results and finite element method results only differ by 5%.

Helical gears have higher load carrying capacities than spur gears because their contact ratios are larger than those of spur gears.

Increasing the helix angle  $\beta$  results in an increase in the axial force  $F_a$ . Thus, one of the disadvantages of increasing the helix angle is the increase of axial forces on the helical gear mechanism.

## Conflicts of Interest

The author declares no conflicts of interest regarding the publication of this paper.

## References

- [1] Bozca, M. (2017) Optimisation of Effective Design Parameters for an Automotive Transmission Gearbox to Reduce Tooth Bending Stress. *Modern Mechanical Engineering*, **7**, 35-56. <https://doi.org/10.4236/mme.2017.72004>
- [2] Ventkatesh, B., Prabhakar, Vattikuti, S.V. and Deva Prasad, S. (2014) Investigate the Combined Effect on Gear Ratio, Helix Angle, Facewidth and Module on Bending and Compressive Stress of Steel Alloy Helical Gear. *Procedia Material Science*, **6**, 1865-1870. <https://doi.org/10.1016/j.mspro.2014.07.217>
- [3] Zhan, J.X. and Fard, M. (2018) Effects of Helix Angle, Mechanical Errors, and Coefficient of Friction on the Time-Varying Tooth-Root Stress of Helical Gears. *Measurement*, **118**, 135-146. <https://doi.org/10.1016/j.measurement.2018.01.021>
- [4] Pedrero, J.I., Pleguezuelos, M. and Munoz, M. (2011) Contact Stress Calculation of Undercut Spur and Helical Gear Teeth. *Mechanism and Machine Theory*, **46**, 1633-1646. <https://doi.org/10.1016/j.mechmachtheory.2011.06.015>
- [5] Kang, J.S. and Choi, Y.-S. (2008) Optimisation of Helix Angle for Helical Gear System. *Journal of Mechanical Science and Technology*, **22**, 2393-2402. <https://doi.org/10.1007/s12206-008-0804-z>
- [6] Juvinall, R.C. and Marshek, K.M. (2006) *Fundamentals of Machine Component Design*. John Wiley & Sons, Inc., Hoboken.
- [7] Norton, R.L. (2011) *Machine Design*. Prentice Hall, Upper Saddle River, NJ.
- [8] ISO 6336-5: Calculation of Load Capacity of Spur and Helical Gears-Part 5: Strength and Quality of Materials.
- [9] ISO 6336-3: Calculation of Load Capacity of Spur and Helical Gears-Part 3: Calculation of Tooth Bending Strength.
- [10] Matek, R. (2005) *Maschinenelemente*. Vieweg & Sohn Verlag/Fachverlage, GmbH, Wiesbaden.
- [11] Decker (2009) *Maschinenelemente*. Carl Hanser Verlag, München.
- [12] Naunheimer, H., Bertsche, B., Ryborz, J. and Novak W. (2011) *Automotive Transmissions*. Springer-Verlag, Berlin, Heidelberg. <https://doi.org/10.1007/978-3-642-16214-5>
- [13] Moaveni, S. (2003) *Finite Element Analysis, Theory and Application with ANSYS*. Prentice Hall, Upper Saddle River, NJ.
- [14] Chandrupatla, T.R. and Belegundu, A.D. (2002) *Introduction to Finite Elements in Engineering*. Prentice Hall, Upper Saddle River, NJ.